~~CONFIDENTIAL~~

Copy 1
RM SE55E23

NACA RM SE55E23

NACA

RESEARCH MEMORANDUM

for the

Bureau of Aeronautics, Department of the Navy

PRELIMINARY RESULTS OF THE DETERMINATION OF INLET-PRESSURE DISTORTION EFFECTS ON COMPRESSOR STALL AND ALTITUDE OPERATING LIMITS OF THE J57-P-1 TURBOJET ENGINE

By L. E. Wallner, R. J. Lubick, and L. J. Chelko

Lewis Flight Propulsion Laboratory
Cleveland, Ohio

NATIONAL ADVISORY COMMITTEE
FOR AERONAUTICS

WASHINGTON

MAY 31 1955

~~CONFIDENTIAL~~

NATIONAL ADVISORY COMMITTEE FOR AERONAUTICS

RESEARCH MEMORANDUM

for the

Bureau of Aeronautics, Department of the Navy

PRELIMINARY RESULTS OF THE DETERMINATION OF INLET-PRESSURE DISTORTION EFFECTS ON COMPRESSOR STALL AND ALTITUDE OPERATING LIMITS OF THE J57-P-1 TURBOJET ENGINE

By L. E. Wallner, R. J. Lubick, and L. J. Chelko

SUMMARY

During an investigation of the J57-P-1 turbojet engine in the Lewis altitude wind tunnel, effects of inlet-flow distortion on engine stall characteristics and operating limits were determined. In addition to a uniform inlet-flow profile, the inlet-pressure distortions imposed included two radial, two circumferential, and one combined radial-circumferential profile. Data were obtained over a range of compressor speeds at an altitude of 50,000 and a flight Mach number of 0.8; in addition, the high- and low-speed engine operating limits were investigated up to the maximum operable altitude. The effect of changing the compressor bleed position on the stall and operating limits was determined for one of the inlet distortions.

The circumferential distortions lowered the compressor stall pressure ratios; this resulted in less fuel-flow margin between steady-state operation and compressor stall. Consequently, the altitude operating limits with circumferential distortions were reduced compared with the uniform inlet profile. Radial inlet-pressure distortions increased the pressure ratio required for compressor stall over that obtained with uniform inlet flow; this resulted in higher altitude operating limits. Likewise, the stall-limit fuel flows required with the radial inlet-pressure distortions were considerably higher than those obtained with the uniform inlet-pressure profile. A combined radial-circumferential inlet distortion had effects on the engine similar to the circumferential distortion. Bleeding air between the two compressors eliminated the low-speed stall limit and thus permitted higher altitude operation than was possible without compressor bleed.

INTRODUCTION

At the request of the Navy Department, Bureau of Aeronautics, an investigation was conducted to determine the steady-state and transient performance of the J57-P-1 turbojet engine in the altitude wind tunnel at the NACA Lewis laboratory. The altitude performance of the engine operating in the steady-state condition is presented in references 1 and 2. Preliminary data on the effects of inlet-pressure distortions on compressor pressure ratios and engine fuel flows, for both the steady-state and stall conditions are presented in references 3 and 4, respectively. This report presents compressor stall limit data for inlet distortions more severe than reported in references 3 and 4. In addition, inlet-distortion effects on the altitude operating limits of the engine are presented. Data are shown for two circumferential and two radial distortions, and for one combined radial-circumferential inlet-pressure distortion.

The operating limits of the engine were determined with each distortion at altitudes above 35,000 feet. This was accomplished by increasing or decreasing engine speed at constant altitude with the compressor bleeds closed until stall of either compressor was obtained. At 50,000 feet, sufficient step increases in fuel flow were also made to determine the compressor stall limits for several of the inlet-pressure distortions. The effect of opening the compressor bleed valves on the altitude operating limits was determined for one inlet-pressure distortion.

APPARATUS

Engine and Installation

A cross-sectional view of the J57-P-1 two-spool turbojet engine is shown in figure 1. The inner spool consists of a seven-stage axial-flow compressor connected by a hollow shaft to a single-stage shrouded turbine. The outer spool consists of a nine-stage axial-flow compressor and a two-stage shrouded turbine connected by a shaft inside of and concentric with the hollow shaft of the inner spool. The sea-level thrust rating of the engine is about 9500 pounds at an inner-spool speed of 9600 rpm and exhaust temperature of 1100° F. The combustor is of the cannular type having eight tubular liners, each with six duplex fuel-spray nozzles.

The engine is equipped with two compressor bleed ports that permit the bleeding of air from the discharge of the outer compressor in order to avoid outer compressor stall at low engine speeds. Opening and closing of the compressor bleeds is scheduled with outer-spool speed and engine-inlet temperature. This schedule is such that bleed actuation occurs between outer spool speeds of about 5000 and 5600 rpm for engine-inlet temperatures of -30° and 120° F, respectively.

The turbojet engine was mounted on a wing section that spanned the test section of the altitude wind tunnel. Atmospheric air was dried, refrigerated, and throttled to the desired pressure level before being supplied to the engine by means of inlet ducting. Automatic bleed valves in the inlet ducting were used to maintain the ram pressure at the desired level during transient engine operation.

Instrumentation

Instrumentation used to measure the steady-state compressor performance is indicated in figure 1. The following parameters were measured on a multiple-channel oscillograph both during steady-state and transient operation: (1) outer and inner compressor speed, (2) inlet and outlet pressures for both outer and inner compressor, (3) inner compressor inlet temperature, and (4) engine fuel flow.

Inlet Distortion Screens

The inlet-pressure distortions were produced by screen segments installed at the engine inlet 13 inches upstream of the inlet guide vanes (fig. 2). In order to support the fine mesh screens, a 1/4-inch-mesh screen was placed over the entire annulus. The uniform inlet total-pressure distribution is therefore the profile existing behind this 1/4-inch-mesh screen. To maintain the total-pressure gradient set up by the radial distortion screen (with a uniform static-pressure profile), an annular ring of 30-mesh screen was placed at the radial boundary of the distortion screen. This screen annulus extended back to the inlet guide vanes as shown in figure 2. The configurations and sizes of the screens are described in the following table and their location shown schematically in figure 3:

Configuration	Type of distortion	Screen size
Undistorted	Uniform	None
A	Radial-1 in. boundary	30 Mesh (wire size, 0.0135 in.)
B	Radial-50 percent area	30 Mesh (wire size, 0.0135 in.)
C	Circumferential-two spot	30 Mesh (0.010 in.) 28×30 mesh (0.0135 in.)
D	Circumferential-graduated	0-10 (0.025 in.)-20(0.017 in.)-30(0.0135 in.) mesh (wire size)
E	Combined radial-circumferential	30 Mesh (0.0135 in.)

PROCEDURE

Steady-state and transient data were obtained with the several inlet-pressure distortions at an altitude of 50,000 feet and 0.8 flight Mach number. The compressor stall characteristics were obtained in the high-speed region with the compressor bleeds manually held in the closed position. For each inlet configuration, the steady-state operating line and the compressor stall line were determined for the engine with rated exhaust-nozzle area. The operating conditions of the compressors at the point where stall was encountered were obtained by using step increases in fuel flow and recording the performance parameters on the transient instrumentation. The step increases in fuel flow were made possible by replacing the standard engine fuel control with a special fuel control.

In addition to the inlet-distortion effects on the compressor stall characteristics at 50,000 feet, distortion effects on the altitude stall limits were determined. These limits were obtained by either increasing or decreasing engine speed with the compressor bleeds closed until stall of either the inner or outer compressor was obtained. However, at high engine speeds, limiting temperature was encountered before steady-state stall. As a result, the steady-state stall limit was found by extrapolating the stall line until it intersected the steady-state operating line.

The graduated circumferential distortion (configuration D) was investigated with the compressor bleeds both open and closed to determine the effect of bleed position on the altitude operating limits of the engine.

RESULTS AND DISCUSSION

Types of Distortion

The shapes and magnitudes of pressure distortion imposed on the engine at the compressor inlet are shown in figures 4 to 6. Data presented in these figures are for an altitude of 50,000 feet and a flight Mach number of 0.8 for all configurations except configuration D. Because the engine was not operable with distortion configuration D at 50,000 feet, the data shown are for an altitude of 35,000 feet and a flight Mach number of 0.8. Both radial distortions resulted in high-pressure regions at the hub and low-pressure regions at the tip of the compressor blades as shown by the curves in figure 4(a). Because the pressure drop across a screen configuration is a function of air flow, the percentage of pressure distortion resulting from the screens increases rapidly with corrected engine speed (fig. 4(b)). At a corrected outer compressor speed of 6200 rpm (about 90 percent rated speed), the two radial distortions investigated had maximum pressure differences of 29 and 19 percent. The maximum pressure difference obtained in reference 3 was only 12 percent for the radial distortion. The pressure gradients of the two circumferential distortions are shown in figure 5. The graduated circumferential distortion, configuration D, was the same as that reported in reference 3. The distortion screens used in configuration C extended only through two 60° arcs, which resulted in two low-pressure areas around the circumference. Configuration E (fig. 6) was similar to radial distortion B except that the distorting screen extended around only one-third of the circumference.

Effect of Distortion on Stall and Operating Limits

The effects of these inlet-pressure distortions on the corrected speed relation between the inner and outer compressor spools for steady-state operation is shown in figure 7. Similar to the distortion data presented in reference 3, the speed relation between the two compressors was unaffected by changes in inlet-pressure distribution.

Uniform inlet-pressure distribution. - Inner- and outer-compressor data with the uniform inlet-pressure distribution and the bleed ports closed is shown by the data in figure 8. On this figure are presented the steady-state operating lines for the two compressors and stall points obtained from either increasing or decreasing engine fuel flow. For the range of data presented, increasing the fuel flow caused inner-compressor stall; whereas, decreasing the fuel flow caused outer-compressor stall. In the range of compressor speeds investigated, compressor stall was followed by engine surge, resulting in large pressure oscillations. Hereinafter, whenever compressor stall is discussed it is implied that engine surge followed.

The intersection of the stall line with the steady-state operating line of the inner compressor establishes the high-speed operating limit of this compressor. The high-speed steady-state operating limit of the engine may either be inner compressor stall or rated exhaust-gas temperature. Generally, rated exhaust temperature was encountered before compressor stall so that some extrapolation was required to determine the high-speed inner compressor stall limit (see intersection on fig. 8(b) and high-speed stall line on fig. 9). The low-speed stall limit was obtained by decreasing engine speed until stall was encountered; this low-speed stall represents the intersection of the steady-state operating line with the stall line of the outer compressor. Stalling of the outer compressor is evidenced by the fact that the pressure ratio of the inner compressor was not increased above the steady-state operating line. This indirect indication of outer compressor stall is resorted to because all operating points lie close to a single line when pressure ratio is plotted as a function of speed (see fig. 8(a)).

The effect of altitude on the stall limits with the compressor bleeds closed is shown by the data in figure 9 for uniform inlet flow. Superimposed on this figure is the speed region at which the inter-compressor bleeds are normally actuated. As demonstrated in reference 5, opening the bleeds eliminates the stall of the outer compressor which constitutes the low-speed limit on this figure. All the high-speed stall points occurred at exhaust-gas temperatures above the recommended operating limit. The band of outer-compressor stall points represents the low-speed operating limit; scatter of points result from the rate of fuel-flow change with which the limit is approached. The slower the rate of approach, the higher the speed will be at which stall commences. For example, with one configuration at 44,000 feet, a 4 percent decrease in fuel flow per second resulted in stall of the outer compressor at about 85 percent speed; when the fuel rate was decreased to 0.7 percent per second, stall was obtained at 88 percent speed. It should be remembered, however, that the bleeds are normally open here, and thus outer compressor stall would generally be avoided. Maximum altitude operation was obtained at about 60,000 feet; the stall lines are not extrapolated to higher altitudes because engine operation here is marginal.

Radial inlet-pressure distortion. - The effects of radial inlet-pressure distortion on compressor operation are shown in figure 10. Performance of the outer compressor (fig. 10(a)) is similar to that obtained for the uniform inlet-pressure profile; that is, the pressure ratio at which the compressor is operating when stall is encountered is very close to steady-state pressure ratio. Although the steady-state pressure ratio of the inner compressor is close to the undistorted operating line, the stall lines for both radial distortions are higher. Evidence of the improvement is shown at other altitudes by the data in figure 11, which compare the altitude operating limits of radial distortion A with that for the uniform inlet-pressure profile. Sufficient analysis of the data has not been done to explain why these radial distortions should improve the inner compressor surge line. The operating speed region with the radial distortion has been broadened considerably over that obtained with uniform inlet-pressure distribution; maximum altitude at which data were obtained was about 62,000 feet and it is apparent that the single-speed altitude ceiling should be several thousand feet higher than that indicated with the uniform inlet-pressure distribution. As noted on figure 11, the maximum total-pressure variation ($\Delta P/P$) was 0.36 at the high-altitude high-speed limit point.

Circumferential inlet-pressure distortion. - As was shown by the data in reference 3, circumferential distortions have a detrimental effect on compressor operation and altitude operating limits for this engine. Circumferential distortion C, which is a profile with two low-pressure regions around the circumference, reduced the stall line of the inner compressor in the high-speed range (fig. 12). In addition, the low-speed limit (stall of the outer compressor) with configuration C is encountered at considerably higher speeds (fig. 12(a)). The effect of these results on restricting the operating limits is shown in figure 13 along with the effects of the graduated circumferential distortion D. The speed limits and maximum operable altitude have been reduced with both circumferential distortions. Configuration D is the same distortion for which the engine was reported to be nonoperable at 50,000 feet in reference 3. The highest altitude at which it was operated during these tests was about 47,000 feet. The high-speed stall limits obtained with this distortion were at exhaust temperatures below the limiting value. Maximum pressure-loss ratio ($\Delta P/P$) was 0.22 for this condition. It should be noted here that stall of the outer compressor would not be eliminated by the normal bleed schedule in the vicinity of 45,000 feet because the compressor is stalling in the speed range where the bleeds would be closed. The operable speed range at lower altitudes was severely restricted compared with the uniform inlet-profile data.

<u>Combined inlet-pressure distortion</u>. - The combined distortion, configuration E, was part radial and part circumferential with the distorting screen extending 120° around the circumference and only across the outer 50 percent of the annulus. The characteristics of this mixed distortion are similar to the circumferential distortions; the high-speed stall line of the inner compressor was lowered somewhat and the outer compressor stalled at a higher engine speed than with the uniform inlet-pressure profile (fig. 14). Altitude operating limits are likewise considerably reduced (fig. 15); the highest altitude at which data were obtained was about 53,000 feet.

Effect of Compressor Bleed on Altitude Operating Limits

Opening the intercompressor bleeds eliminated the stalling of the outer compressor as demonstrated in reference 5. The effect of opening the bleeds on altitude operation with circumferential distortion D is presented in figure 16. Superimposed on this figure is the operable region with the compressor bleeds closed as was shown in figure 13. Ignoring the normal bleed schedule and operating the engine over the entire speed range with the bleeds open eliminate the low-speed stall limit. Therefore, the only stall limit encountered is high-speed stall of the inner compressor, which occurs at approximately the same speed as with the compressor bleeds closed.

Effect of Pressure Distortion on Steady-State and Stall Fuel Flows

Engine fuel flows required to cause compressor stall are compared with the steady-state values for several inlet-pressure distributions in figure 17. For the uniform inlet-pressure distribution, fuel-flow increases of 100 percent and 40 percent were required for compressor stall at inner-spool corrected speeds of 9000 and 10,000 rpm, respectively. The fuel flows required for compressor stall with the radial pressure distortions are considerably higher than with the uniform pressure distribution. This is further evidence of the increase in acceleration margin that was demonstrated in figure 10(b) and the improvement in altitude operating limits in figure 11. Compressor-stall fuel flows with the circumferential distortion C are slightly reduced from the undistorted stall fuel flows. This also is similar to the pressure-ratio margin as shown by the data in figure 12.

CONCLUDING REMARKS

Circumferential inlet-pressure distortions lower the inner-compressor pressure-ratio margin between the steady-state and stall condition compared to that with uniform flow. Radial inlet-pressure distortions have the opposite effect; the inner-compressor pressure-ratio margin is improved compared with that with the uniform inlet profile. When the pressure-ratio margin of the inner compressor was affected by inlet-pressure distortions, the engine fuel-flow margin and the altitude operating limits were affected in the same direction. The high-speed steady-state operating limit of the engine was rated exhaust-gas temperature except in the case of the graduated circumferential distortion, where inner-compressor steady-state stall was encountered before limiting exhaust-gas temperature. This distortion, which had a maximum total-pressure variation of 0.22 at 0.97 rated engine speed, lowered the maximum operable altitude to 47,000 feet compared with 60,000 feet with uniform inlet flow. Except in the case of the circumferential distortions at high altitude, normal actuation of the inner-compressor bleed ports effectively eliminated stalling of the outer compressor. In general, a combined circumferential-radial inlet-pressure distortion has the same characteristics as a circumferential distortion.

Lewis Flight Propulsion Laboratory
National Advisory Committee for Aeronautics
Cleveland, Ohio, May 23, 1955

REFERENCES

1. Miller, Robert R., and Bloomer, Harry E.: Preliminary Performance Data for the J57-P-1 Turbojet Engine at Altitudes up to 65,000 Feet. NACA RM SE54E26, 1954.

2. Bloomer, Harry E., and Miller, Robert R.: Preliminary Altitude Performance Characteristics of the J57-P-1 Turbojet Engine with Fixed-Area Exhaust Nozzle. NACA RM SE54D30, 1954.

3. Wallner, Lewis E., Lubick, Robert J., and Einstein, Thomas H.: Preliminary Data on the Effects of Inlet Pressure Distortions on the J57-P-1 Turbojet Engine. NACA RM SE54K19, 1954.

4. Lubick, Robert J., Meyer, William R., and Wallner, Lewis E.: Preliminary Data on the Effects of Altitude and Inlet-Pressure Distortions on Steady-State and Surge Fuel Flow of the J57-P-1 Turbojet Engine. NACA RM SE55A06, 1955.

5. Wallner, Lewis E., and Saari, Martin J.: Preliminary Altitude Operational Characteristics of a J57-P-1 Turbojet Engine. NACA RM SE54C31, 1954.

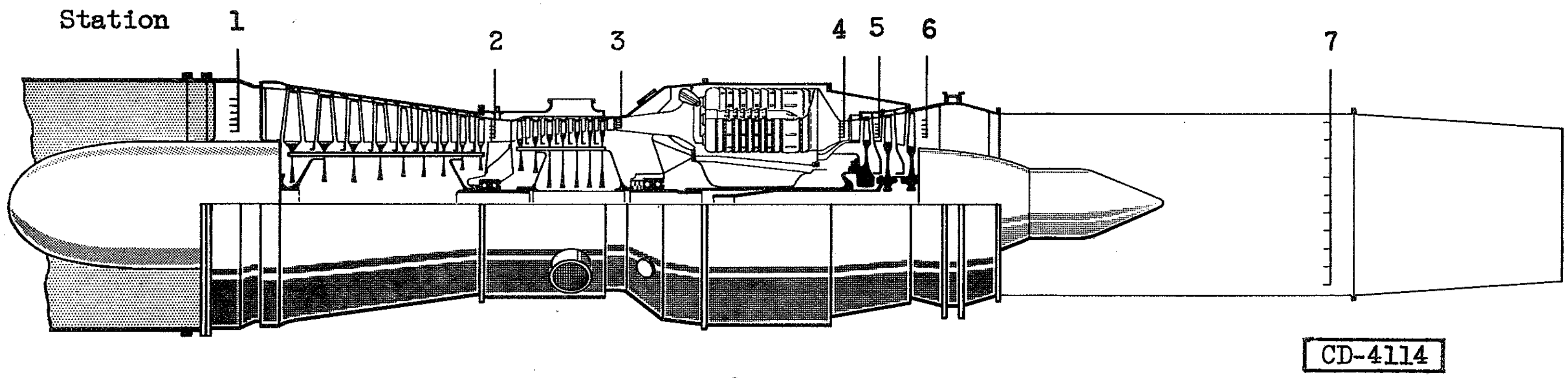

Station	Number of total pressure probes	Number of static pressure probes	Number of thermocouple probes
1	42	16	16
2	24	-	12
3	20	-	12
4	18	-	8
5	16	-	-
6	24	8	24
7	24	4	24

Figure 1. - Schematic diagram of J57-P-1 turbojet engine showing location and amount of steady-state instrumentation.

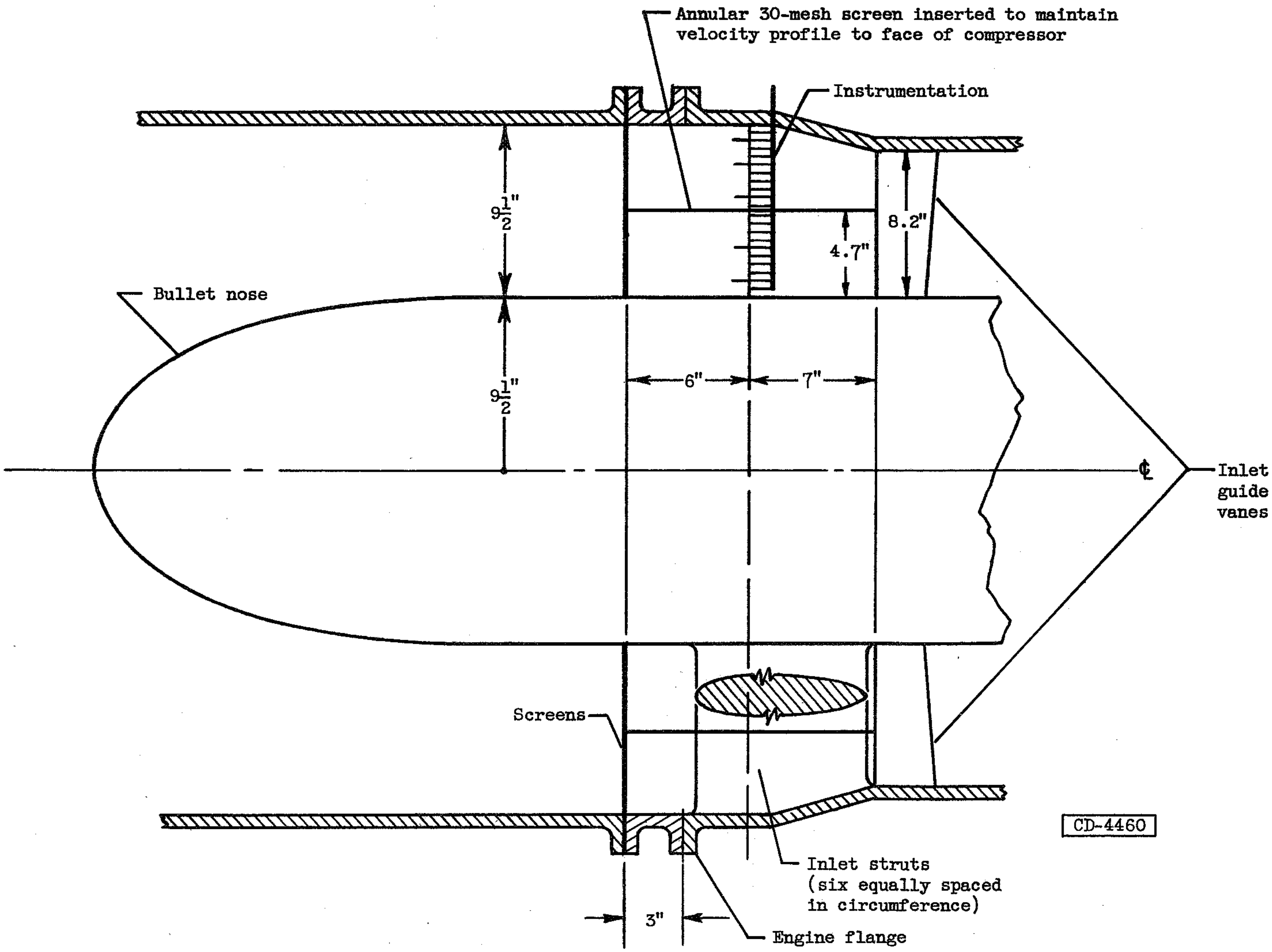

Figure 2. - Location of distortion screens and inlet instrumentation.

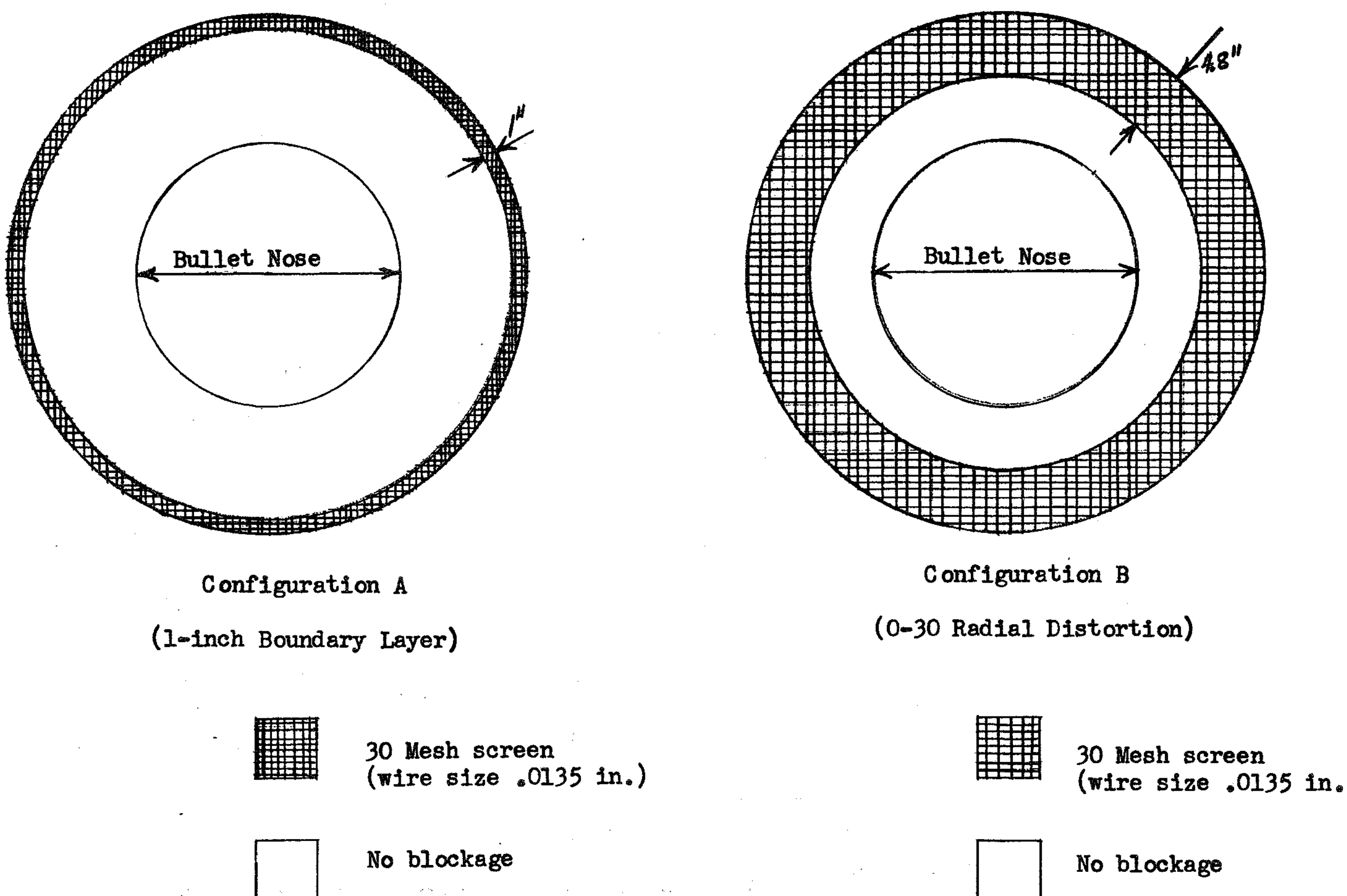

Figure 3. - Sketch of screen segments for inlet distortion investigation
(Note: Distortion screens were supported on a 1/4-inch mesh which spanned the inlet annulus.)

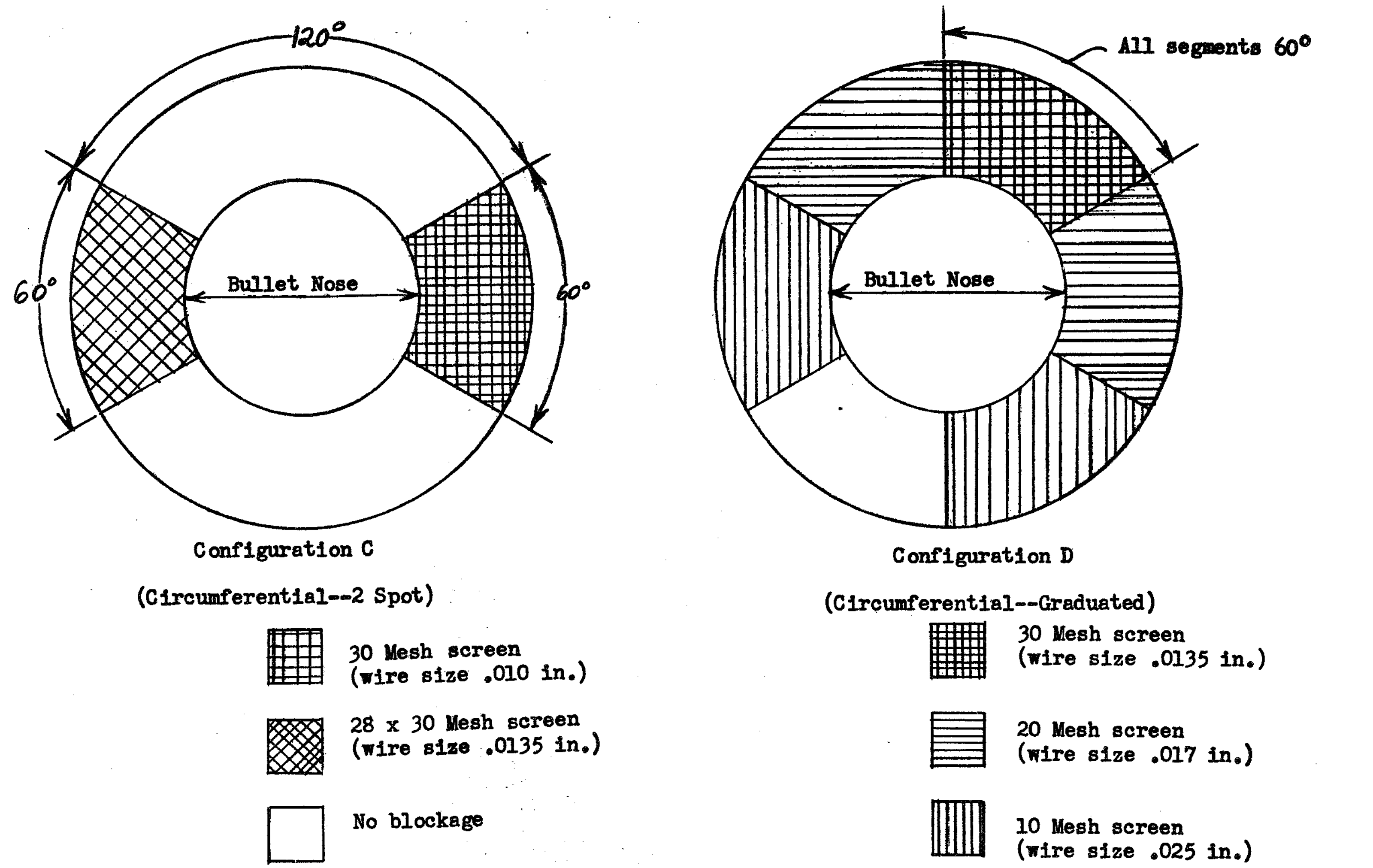

Figure 3. - Continued. Sketch of screen segments for inlet distortion investigation. (Note: Distortion screens were supported on a 1/4-inch mesh which spanned the inlet annulus.)

[redacted]

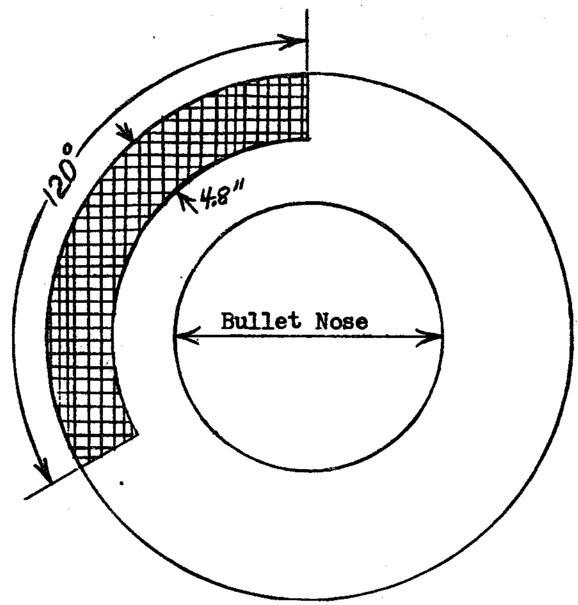

Configuration E

(Combined Radial-Circumferential)

30 Mesh screen
(wire size .0135 in.)

No blockage

Figure 3. - Concluded. Sketch of screen segments for inlet distortion investigation. (Note: Distortion screens were supported on a 1/4-inch mesh which spanned the inlet annulus.)

[redacted]

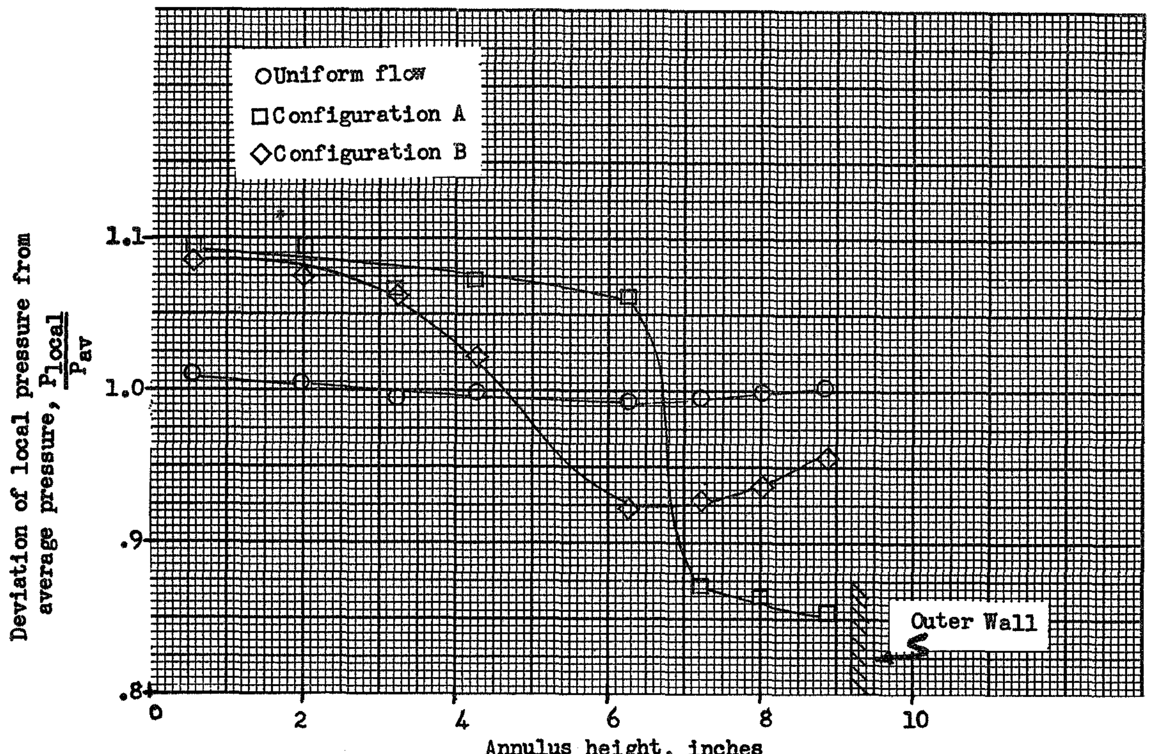

Figure 4(a). - Typical radial inlet pressure profiles. Corrected engine speed, 100 percent of rated

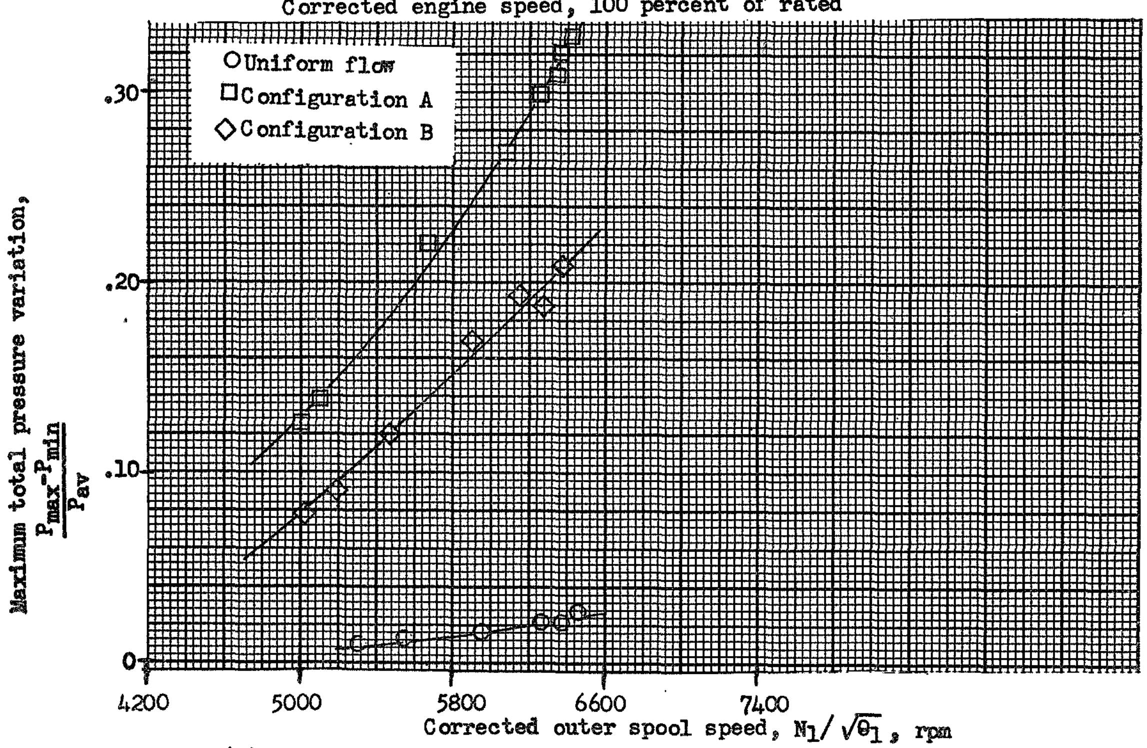

Figure 4(b). - Effect of outer spool corrected speed on the radial total pressure gradients. Altitude, 50,000 feet. Flight Mach number 0.8.

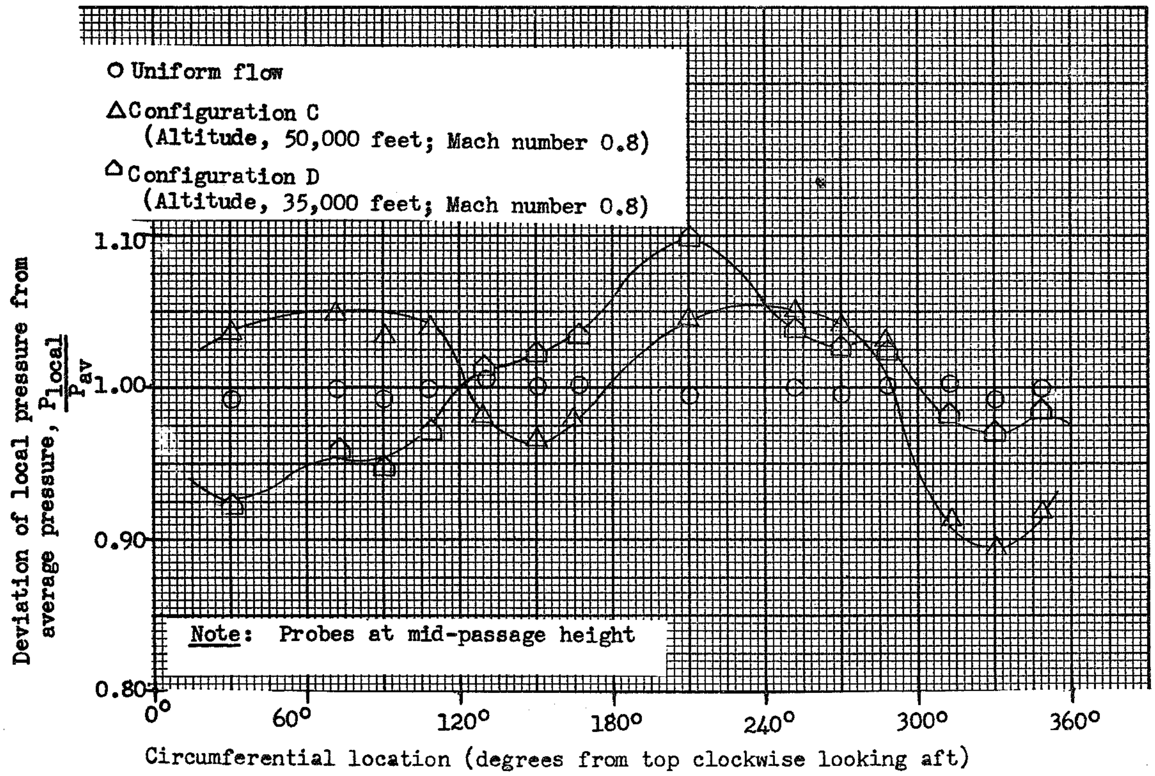

Figure 5(a). - Typical circumferential inlet pressure profiles. Corrected engine speed , 100 percent of rated.

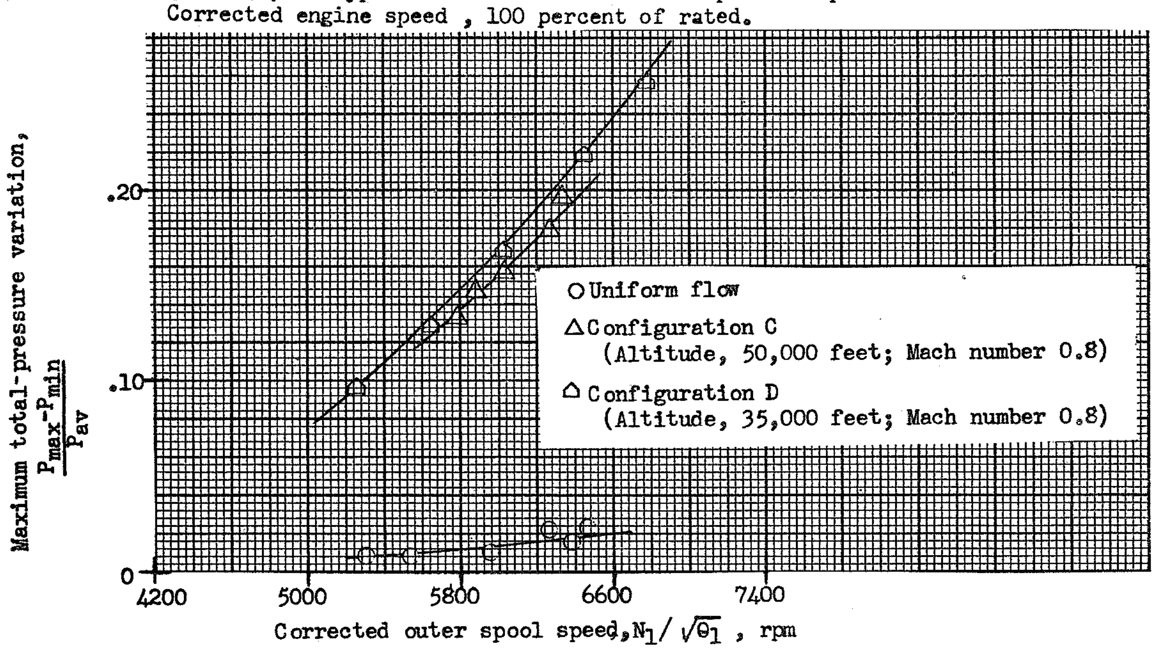

Figure 5(b). - Effect of outer spool corrected speed on the circumferential total pressure gradients.

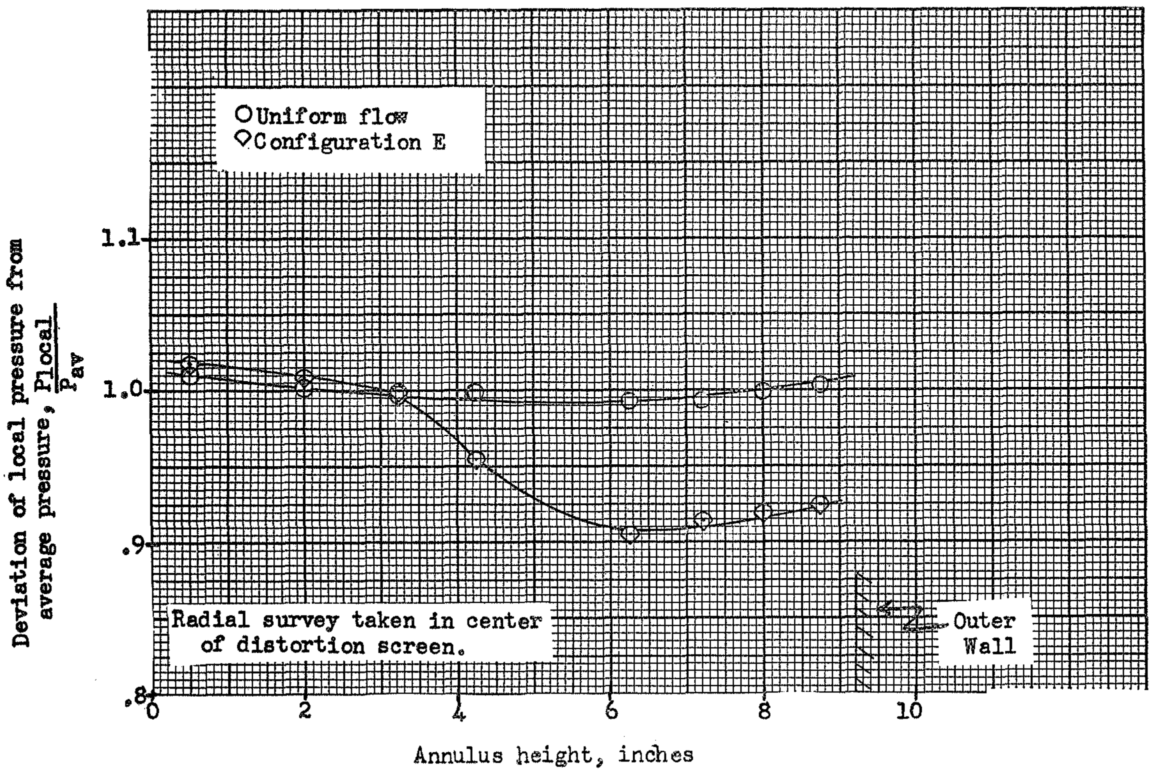

Figure 6(a). - Typical combined radial and circumferential inlet pressure profiles. Corrected engine speed, 100 percent of rated.

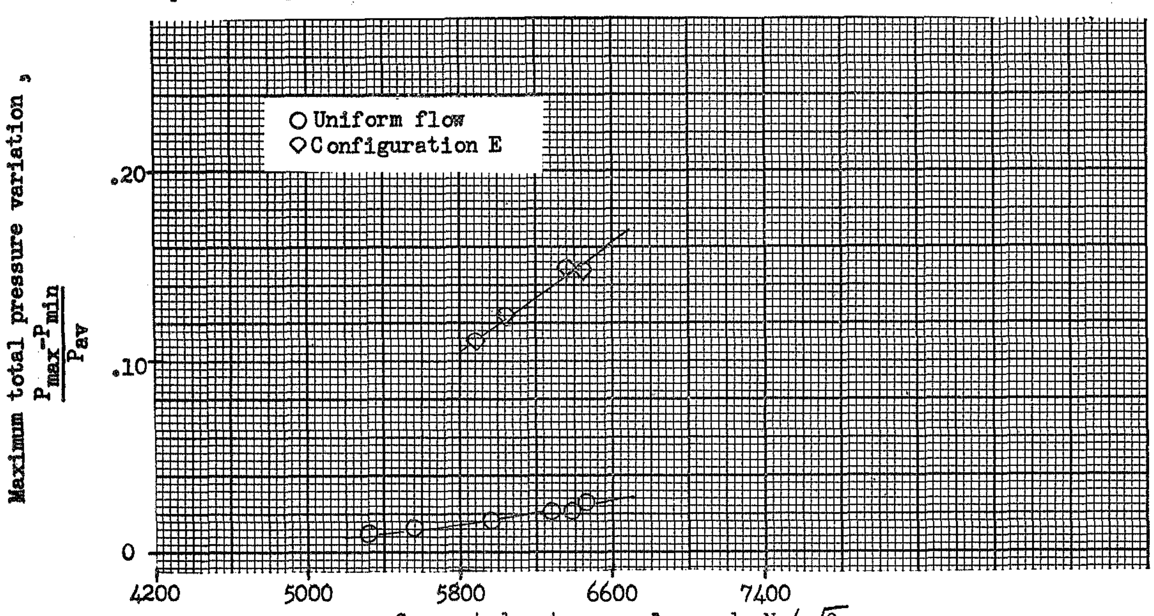

Figure 6(b). - Effect of outer spool corrected speed on the combined radial and circumferential total pressure gradients. Altitude, 50,000 feet. Flight Mach number 0.8.

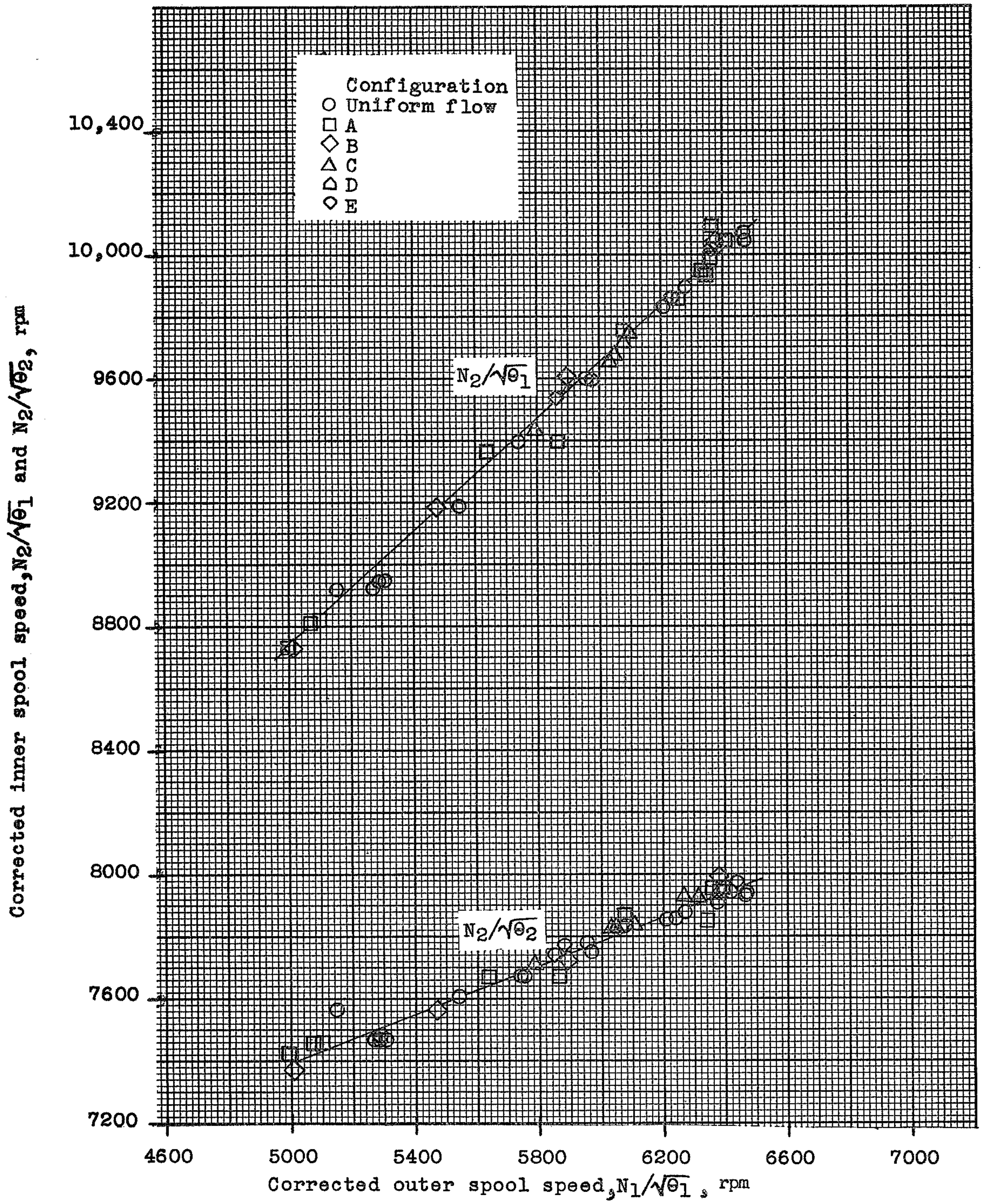

Figure 7. - Variation of corrected inner spool speed with corrected outer spool speed for several inlet distortions. Altitude, 50,000 feet, Mach number 0.8, compressor bleeds closed.

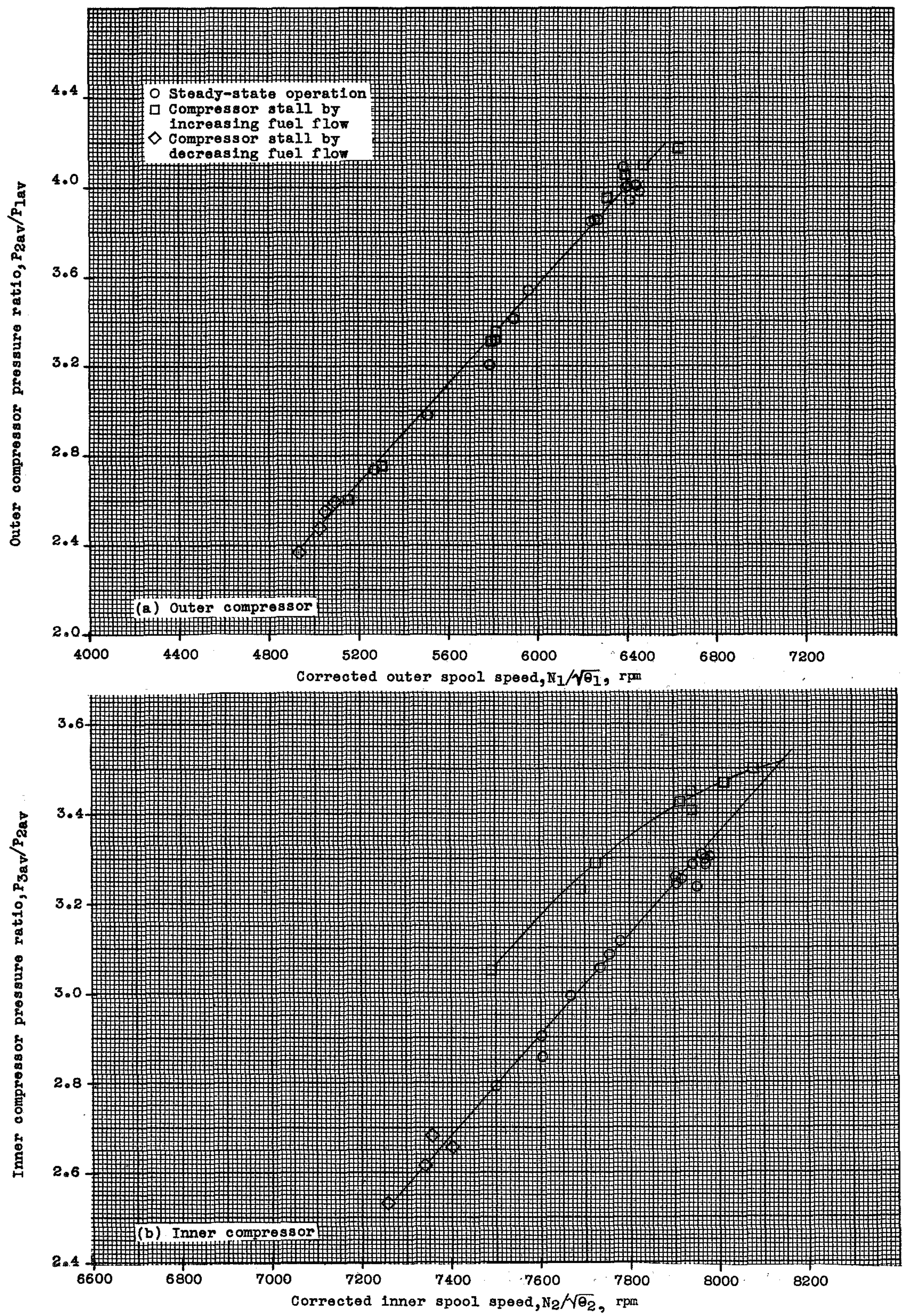

Figure 8. - Stall and steady-state operating lines for inner and outer compressors of J57-P-1 engine operating with uniform inlet pressure distribution. Altitude 50,000 feet, flight Mach number 0.8, compressor bleeds closed.

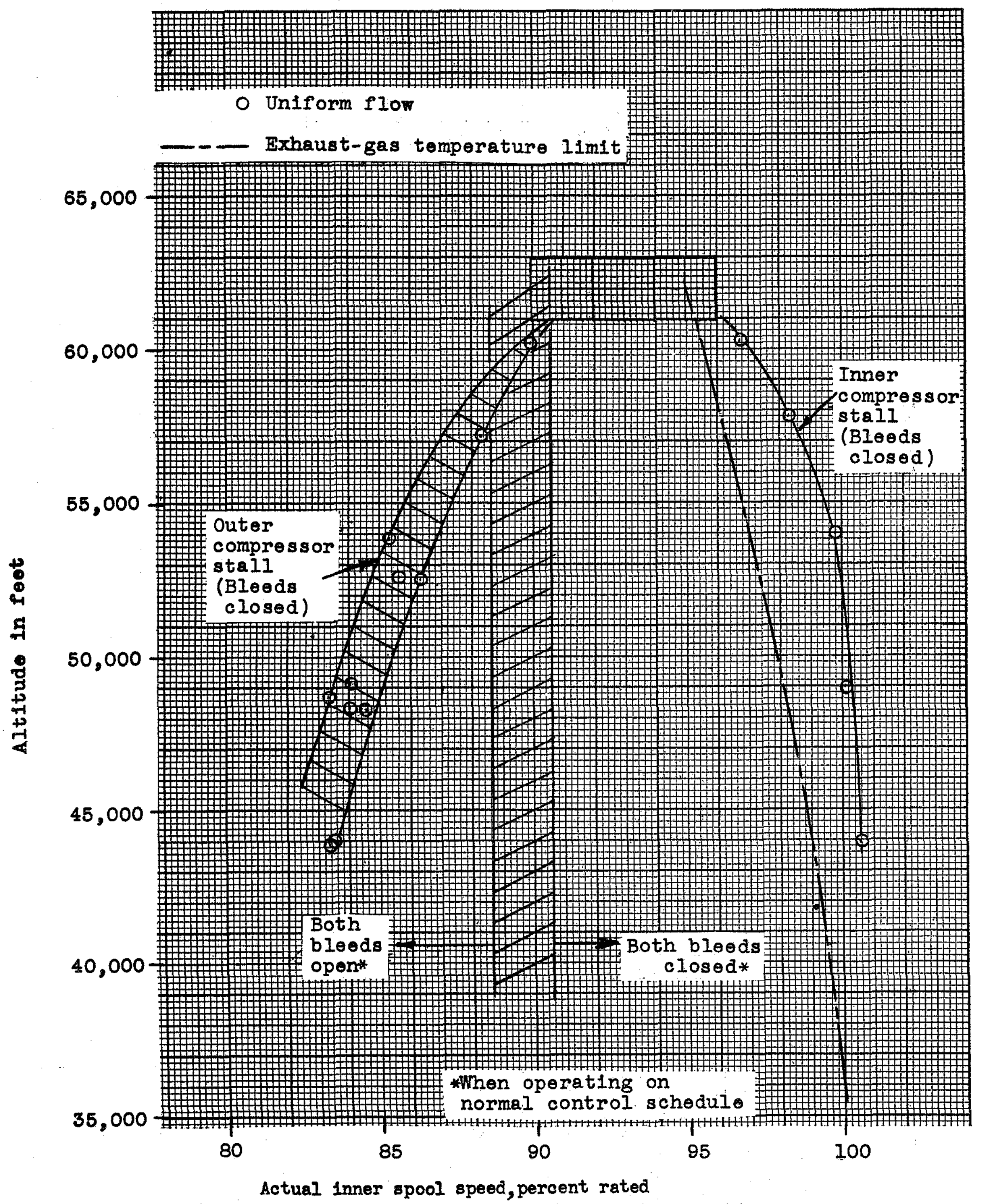

Figure 9. - Effect of altitude on J57-P-1 engine operating limits with uniform inlet pressure distribution. Flight Mach number 0.8, Engine inlet temperature -17° F.

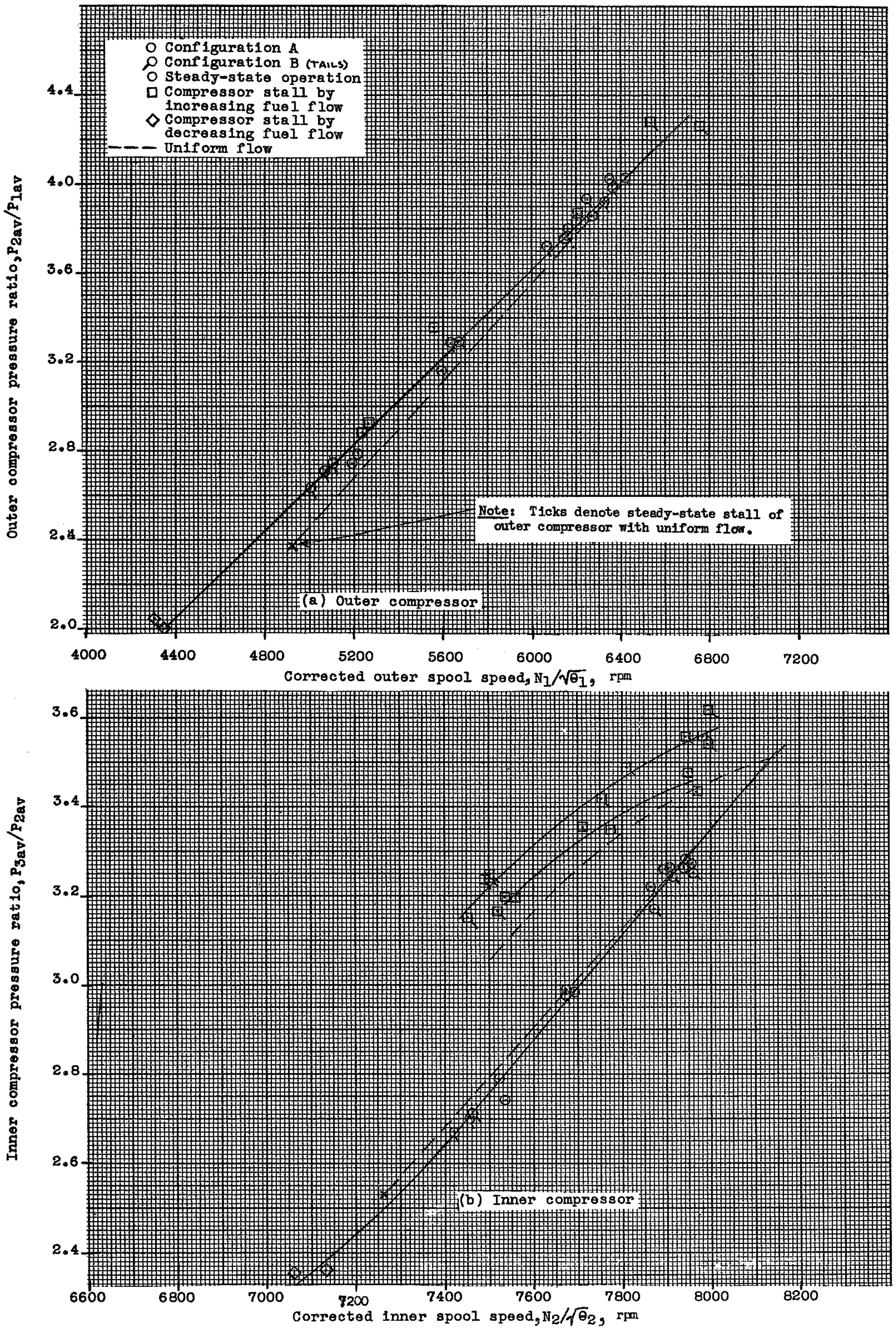

Figure 10. - Stall and steady-state operating lines for inner and outer compressor of J57-P-1 engine with radial pressure distortions. Altitude 50,000 feet, flight Mach number 0.8, compressor bleeds closed.

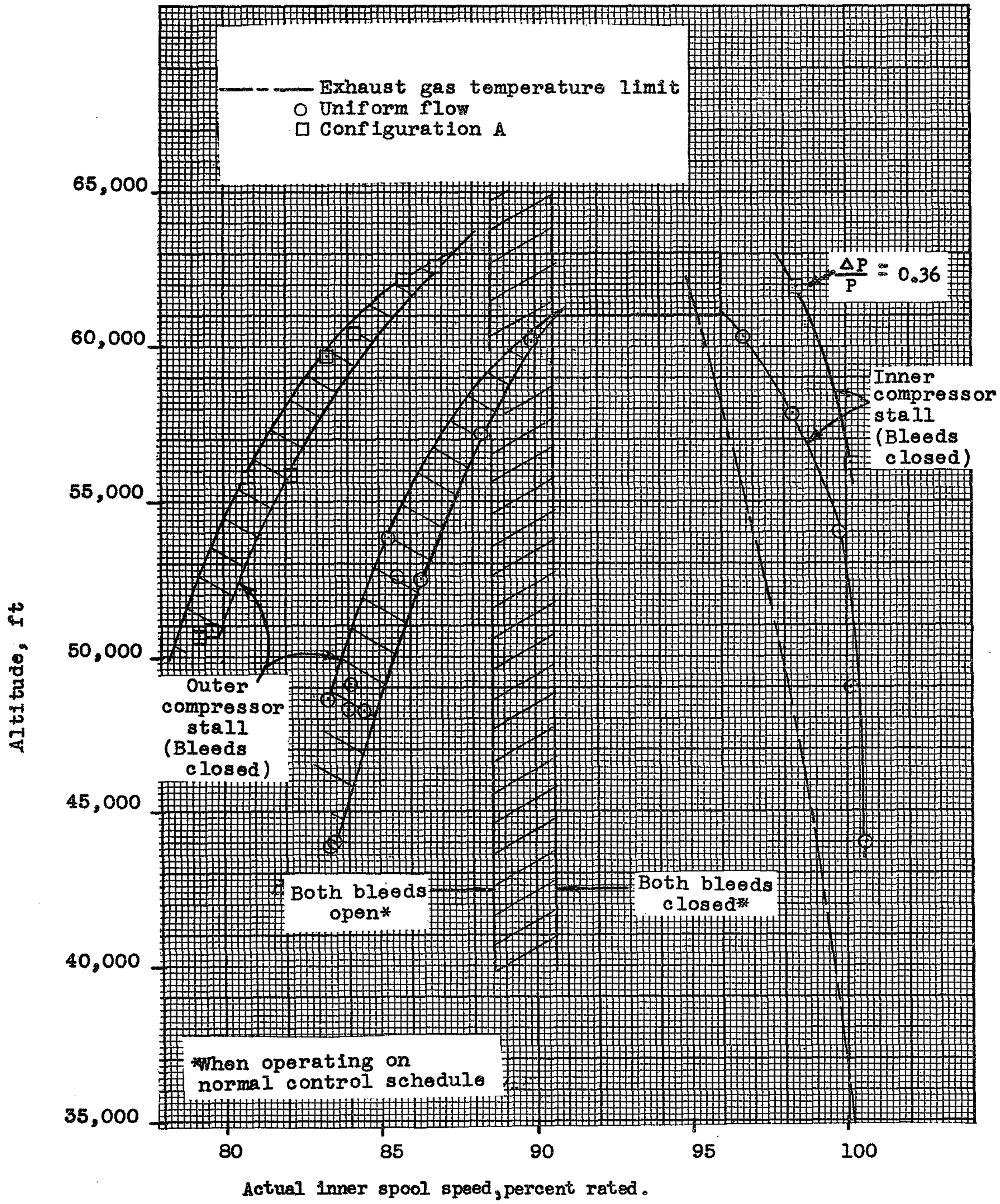

Figure 11. - Effect of altitude on J-57-P-1 engine operating limits with radial inlet pressure distortions. Flight Mach number 0.8; engine inlet temperature, -17° F.

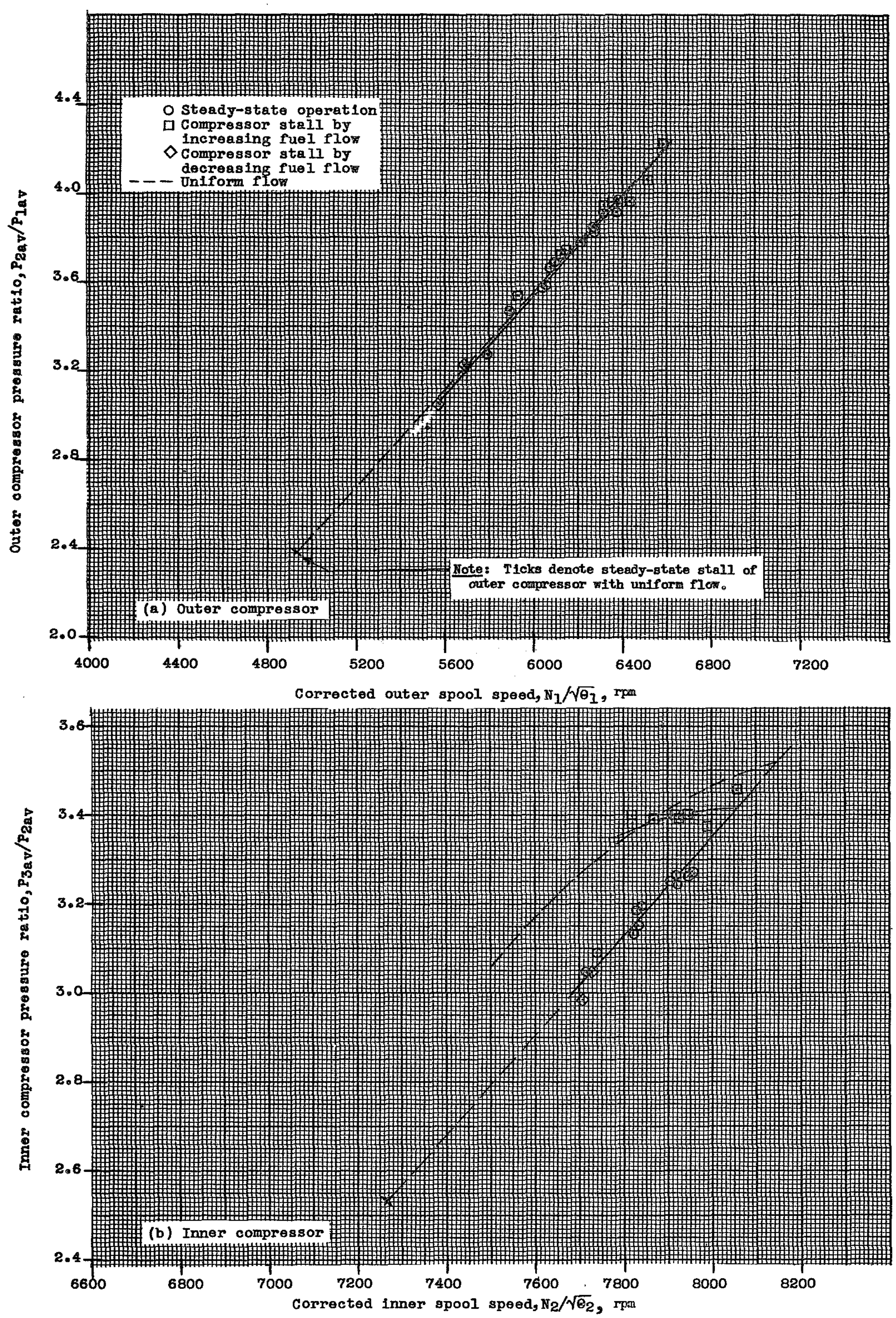

Figure 12. - Stall and steady-state operating lines for inner and outer compressors of J57-P-1 engine with circumferential inlet pressure distortion C. Altitude 50,000 feet, flight Mach number 0.8, compressor bleeds closed.

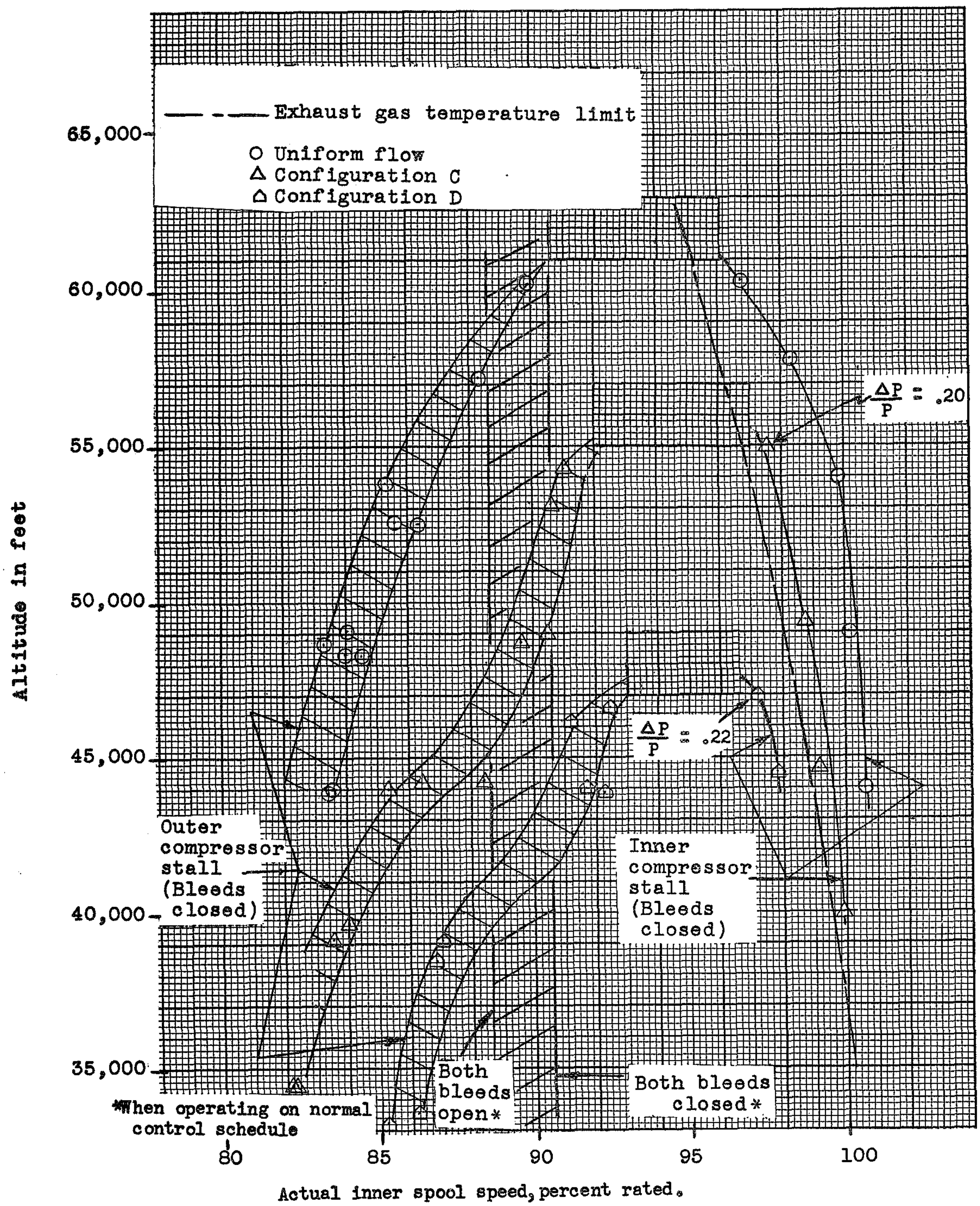

Figure 13. - Effect of altitude on J-57 -P-1 engine operating limits with circumferential inlet pressure distortions. Flight Mach number 0.8, engine inlet temperature -17° F.

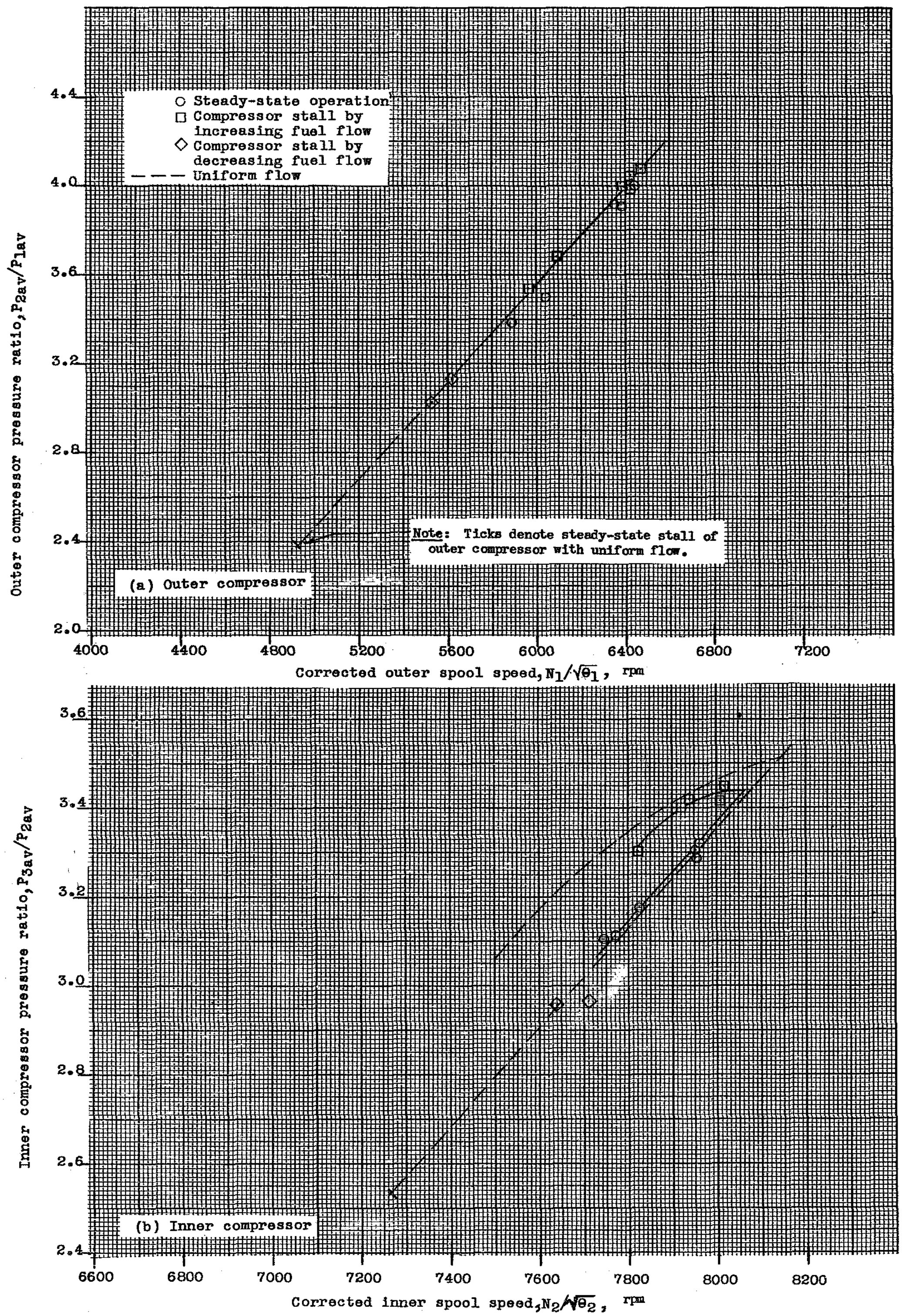

Figure 14. - Stall and steady-state operating lines for inner and outer compressors of J57-P-1 engine with combined circumferential and radial inlet pressure distortion. Altitude 50,000 feet, flight Mach number 0.8, compressor bleeds closed.

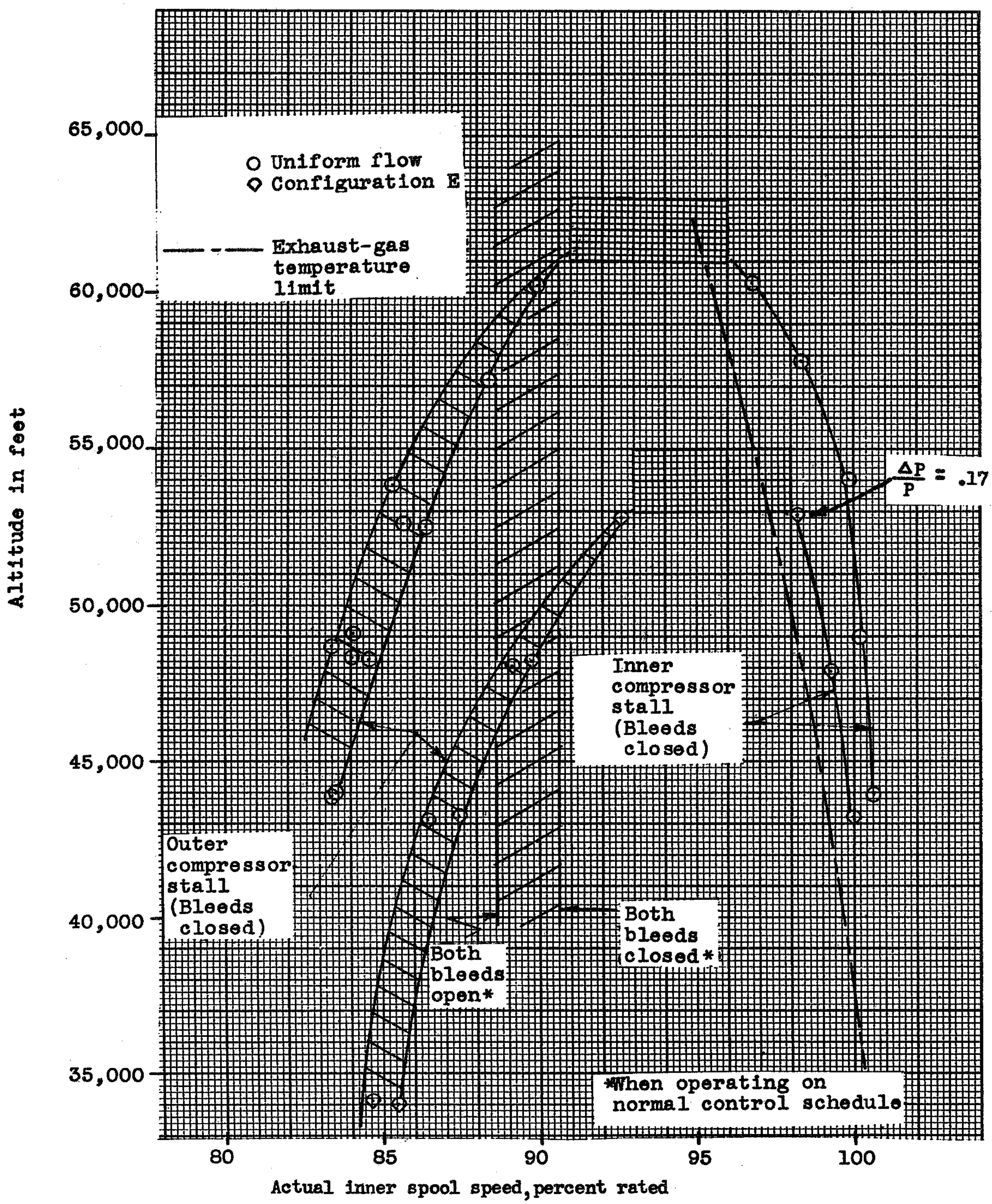

Figure 15. - Effect of altitude on J57-P-1 turbojet engine operating limits with combined circumferential and radial inlet pressure distortions. Flight Mach number 0.8, engine inlet temperature -17° F.

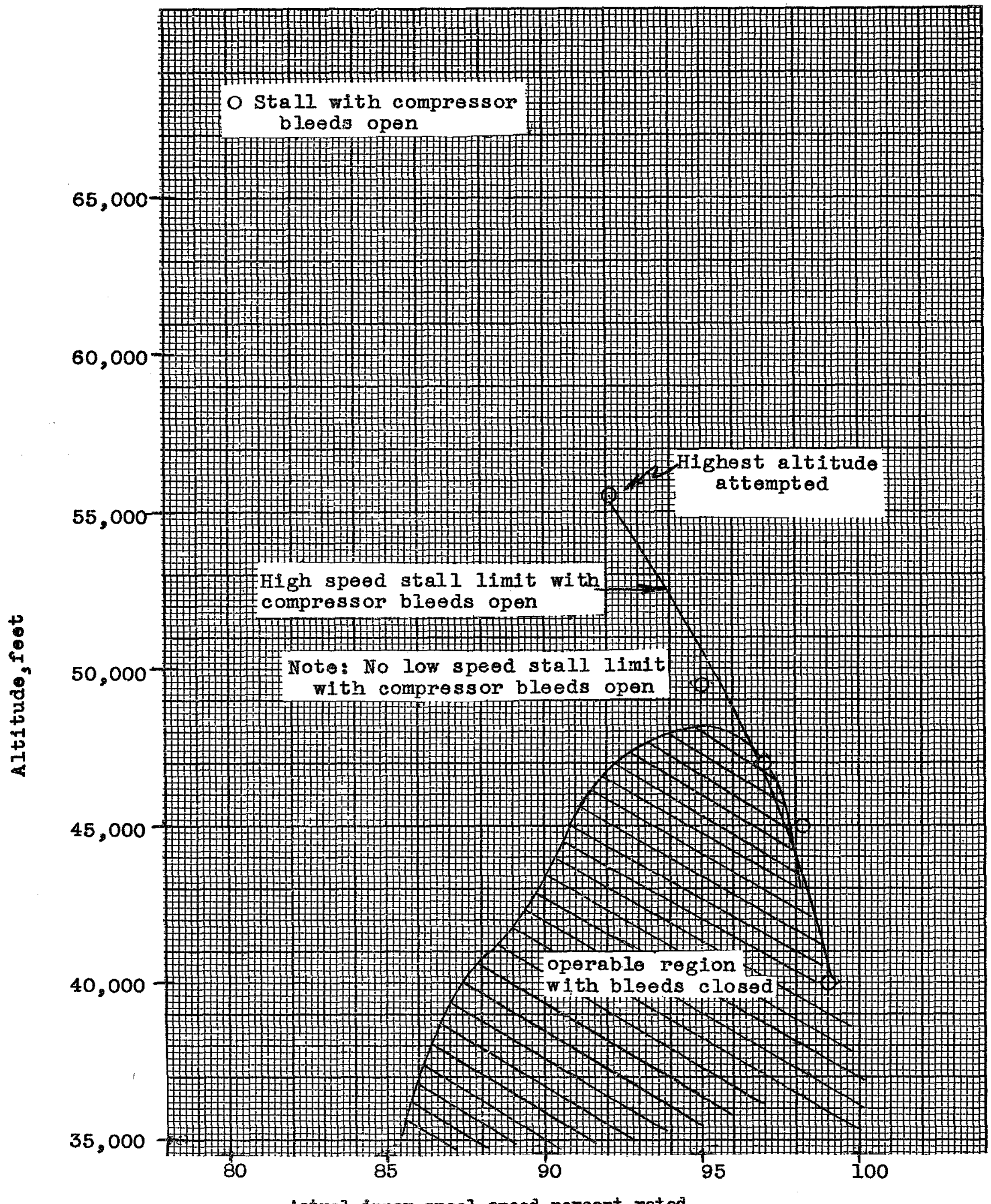

Figure 16. - Effect of compressor bleed on altitude operating limits. Circumferential distortion D. Flight Mach number 0.8, engine inlet temperature -17° F.

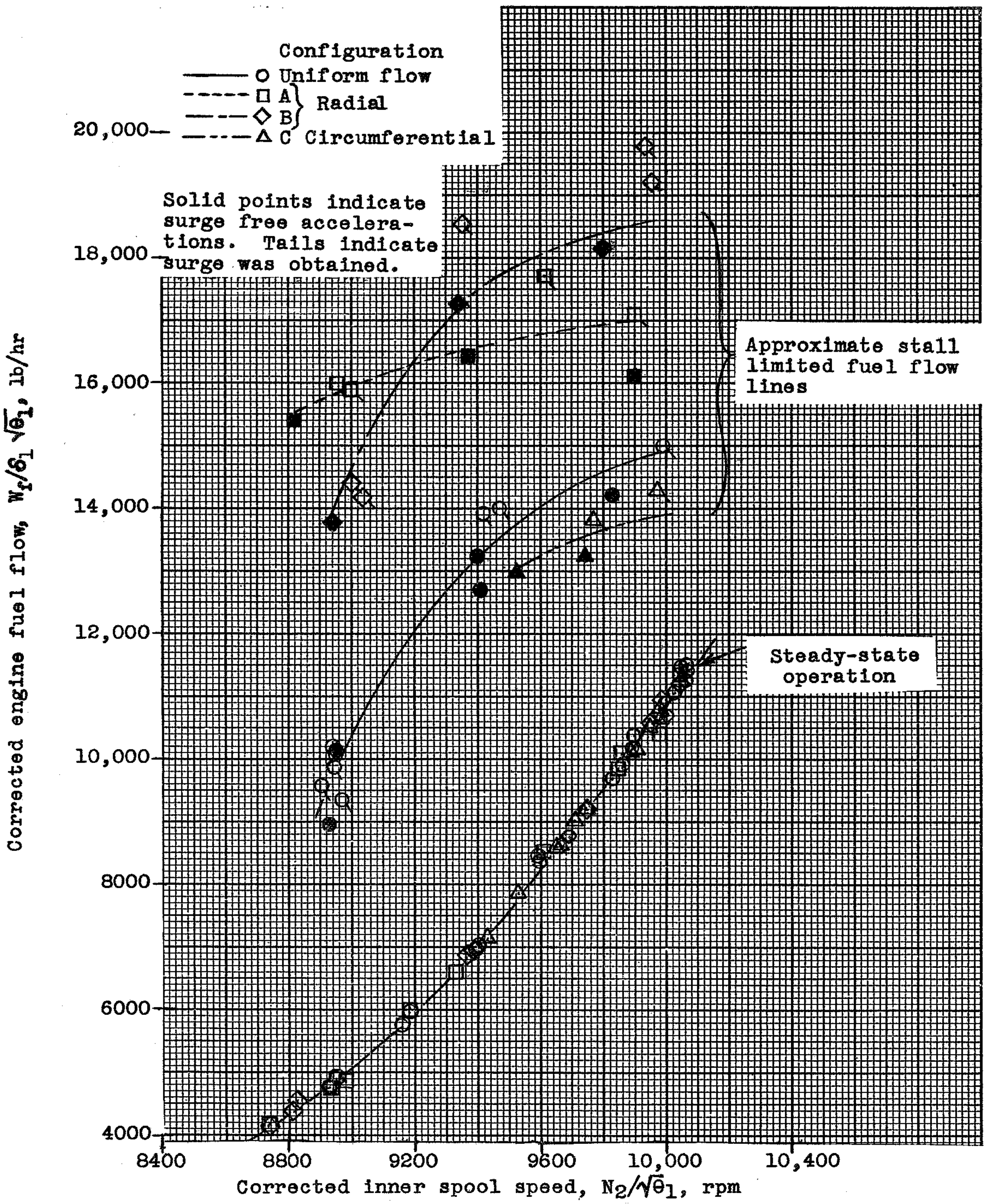

Figure 17. - Effect of inlet pressure distortion on engine fuel flow stall limits. Altitude 50,000 ft, flight Mach number 0.8. Compressor bleeds closed.

NACA RM SE55E23 [redacted]

PRELIMINARY RESULTS OF THE DETERMINATION OF INLET-PRESSURE DISTORTION EFFECTS ON COMPRESSOR STALL AND ALTITUDE OPERATING LIMITS OF THE J57-P-1 TURBOJET ENGINE

Lewis E. Wallner
Aeronautical Research Scientist
Propulsion Systems

Robert J. Lubick
Aeronautical Research Scientist
Propulsion Systems

Louis J. Chelko
Aeronautical Research Facilities Engineer

Approved:

William A. Fleming
Aeronautical Research Scientist
Propulsion Systems

Bruce T. Lundin
Chief
Engine Research Division

mm - 5/23/55

[redacted]